SIMULTANEOUS IMAGE DE-NOISING AND REGISTRATION USING GRAPH CUTS: APPLICATION TO CORRUPTED MEDICAL IMAGES

Herve Lombaert, Farida Cheriet

École Polytechnique de Montréal, Montréal Québec, Canada

ABSTRACT

The success of medical image de-noising often relies on the image quality. If the image is severely degraded, information can be permanently lost. The de-noising or restoration process rarely use any other external information such as valuable data from additional images, for instance from a follow-up study or within an image sequence. Several optimization methods exist, among them the Graph Cuts method is efficient in a global optimum sense. We show that Graph Cuts can be used to solve simultaneously image de-noising and image correspondence. Both of these problems have been previously solved with Graph Cuts, but always as separate processes. In this paper, we combine them in the same formulation, and we show an application where images, initially unusable, can be recovered rather than being reacquired at a high risk (e.g., avoiding new radiation in medical scans).

1. INTRODUCTION

Medical images, as observed, usually present a certain level of degradation due to the environment during acquisition or to the physics underlying the image formation, sometimes so severe that information can be lost in the image. The recovery of the original, or ideal, image is known as the restoration process. Most general information can be recovered from observed images, however, depending on the degradation severity, details such as the precise location of organ boundaries, thin vessels, or poorly contrasted structures can be permanently lost, and might require a costly reacquisition of the image. This is undesirable when dealing with radiation in medical imaging. However, in addition to the low quality image, a second image with a better quality is sometimes available. It can be an image of the same patient taken on a different day, another frame from an image sequence, or an image taken in a modality yielding less noise. This second image provides valuable additional information that helps the recovery of a severely degraded image.

Image de-noising is a nonlinear inverse problem, and since the beginning of computer vision [1], relationships between pixels have been exploited. In the early days, Geman and Geman [2] used in a Bayesian framework *a priori* knowledge on the distribution of neighboring structures. Since then, other popular approaches for image de-noising and enhancement have been used [3, 4, 5]. They are often formulated in a variational framework and prone to local minima. In this paper, we focus on the Graph Cuts approach. Indeed, with particular objective functions, the Graph Cuts have the advantage of finding a solution guaranteed to be in the vicinity of the global minimum [6]. Image restoration via Graph Cuts can be modeled as finding a piecewise smooth function [6, 7] and can be tackled through a statistical approach [8].

Joint approaches allow the combination of two problems within the same optimization formulation. Brailean and Katsaggelos [9] already sensed the relevance of such approaches and were able to enhance restoration by simultaneously estimating the displacement field within an image sequence. Woods *et al.* [10] used a stochastic framework to create a high resolution image from multiple low-quality images. Simultaneous approaches [11, 12] also involve motion segmentation rather than displacement estimation. Recently [12, 13, 14], edge detection is used jointly with the image de-noising and motion segmentation processes.

We show in this paper that a joint approach can be used with Graph Cuts and enhance image restoration. Image de-noising was one of the first Graph Cuts applications, and it has recently been shown that Graph Cuts can be used for image registration [15, 16, 17, 18, 19, 20, 21]. We propose a joint approach, where image de-noising helps the registration process, and the good overlap of a clearer image improves de-noising of a corrupted image. This method can be used in any situations where degraded images need to be restored and when at least one clear image is available. Typical applications include the recovery of a corrupted frame in a sequence, for instance when the imaging device failed for one image acquisition. The sequence could be a short animation (e.g., a cardiac sequence), or different images taken days apart (e.g., monitoring a pathology evolution). In the following, we first remind how Graph Cuts are used to solve image de-noising, and how it can recover deformation fields. Later, we show that both problems can be combined in the same formulation. The results show that a corrupted image, even in an extreme case with missing parts, can indeed be recovered with the registration of an additional image.

2. RESTORATION VIA REGISTRATION

Optimization of submodular functions can be done via Graph Cuts, more specifically with the α-expansion algorithm as described by Boykov *et al.* [6]. Many problems in computer vision can thus be solved via this opti-

mization method, including image de-noising and recovery of deformation fields. After a brief reminder of the optimization framework, the objective functions for image de-noising and registration will be presented, followed by how to combine both formulations in a joint approach.

2.1. Image De-noising

The Graph Cuts algorithm finds the global solution of a binary problem. It finds the minimum cut between a sink and a terminal. For instance, in image segmentation, the minimum cut optimally separates the image foreground from its background. However, when a pixel can be assigned to many labels, $f_p \in \mathcal{L}_f$, a series of Graph Cuts can be used to minimize the following type of energy:

$$E(f) = \sum_{p \in I} D(i_p, f_p) + \lambda \sum_{p,q \in \mathcal{N}} V(f_p, f_q). \qquad (1)$$

The first term is known as the energy of the data term D. It penalizes the current labeling f if it is too different from the observed pixel intensity i in image I. The second term is the energy of the smoothness term V, controlled by the parameter λ. It penalizes the labeling f if it is not smooth enough, that is, if the labels of two neighboring pixels, f_p and f_q, are too different.

Boykov *et al* [6] show two algorithms based on Graph Cuts: the α expansion and the $\alpha - \beta$ swap. They minimize any energy (Eq. 1) whose smoothness term satisfies certain conditions, namely, $V(\alpha, \beta) = 0 \Leftrightarrow \alpha = \beta, V(\alpha, \beta) = V(\beta, \alpha) \geq 0, V(\alpha, \beta) \geq V(\alpha, \gamma) + V(\gamma, \beta)$ with $\alpha, \beta, \gamma \in \mathcal{L}_f$.

The main idea of the α expansion algorithm is to iteratively minimize the energy, testing one label $\alpha \in \mathcal{L}_f$ at a time. In image de-noising, α is a recovered intensity, e.g., $\mathcal{L}_f = [0..255]$. During an algorithm step, a new label $\alpha \in \mathcal{L}_f$ is tested. A Graph Cuts partitions the image in two regions: the α region, where pixels should be assigned the intensity $f_p = \alpha$, and the $\bar{\alpha}$ region, where pixels should remain unchanged. At each new step, the α region is said to expand. The recovered image f is thus optimized while iterating a few times all possible intensities α.

For image de-noising, the data term in (Eq. 1) is designed to assign a recovered intensity, f_p, as close as possible as the observed intensity i_p, for instance, the squared difference is used, $D(i_p, f_p) = (i_p - f_p)^2$. The smoothness term is designed to yield similar intensities between neighboring pixels, for instance, the absolute difference is used, $V(f_p, f_q) = |f_p - f_q|$. The energy as formulated in (Eq. 1) now becomes:

$$\begin{aligned} E(f) &= \sum_{p \in I} (i_p - f_p)^2 \\ &+ \lambda \sum_{p,q \in \mathcal{N}} |f_p - f_q|. \end{aligned} \qquad (2)$$

2.2. Deformation Field Recovery

For the recovery of a deformation field, the inputs are two observed images, I_1 and I_2, the solution is the deformation field, u, and the label set contains all possible deformations, e.g., $\mathcal{L}_u = \{(-10; -10), (-10; -9), ..., (+10; +10)\}$. The same optimization framework described earlier is also used to find the deformation field u. Indeed, the deformation field undergoes two forces, one that matches the warped image I_2 with the original image I_1, the second that keeps the deformation field smooth. These two forces correspond to the data term and the smoothness term in the energy (Eq. 1).

It is assumed that each pixel of an image has a corresponding pixel in the second image, i.e., $I_1(p) \Leftrightarrow I_2(p + u_p)$, where u_p is the displacement between the two pixels. The data term measures how the data differs between the original image and the warped image, for instance with the squared difference of the intensities, $D(I_1(p), I_2(p + u_p)) = (i_1(p) - i_2(p + u_p))^2$. Mutual information [22] can be used when using multimodal images.

The deformation field is also assumed to be locally coherent, i.e., $u_p \approx u_q$, for two neighboring pixels $p, q \in \mathcal{N}$. The smoothness term measures how smooth the deformation is, for instance with the norm of the difference between two neighboring displacements, $V(u_p, u_q) = ||u_p - u_q||$.

Finding a smooth deformation field, u, between two images, I_1 and I_2, is therefore solved by minimizing the following energy:

$$\begin{aligned} E(u) &= \sum_{p \in I_1, I_2} (i_1(p) - i_2(p + u_p))^2 \\ &+ \lambda \sum_{p,q \in \mathcal{N}} ||u_p - u_q||. \end{aligned} \qquad (3)$$

2.3. Joint Approach

In a joint approach the registration brings additional information to the de-noising process. When two images are correctly aligned, the enhancement of the degraded image can benefit from the better quality of the aligned image. Similarly, when the degraded image is enhanced, correspondences between both images become clearer. Both processes can thus benefit from each other in a simultaneous manner. The resulting coherence is the motivation for a joint approach. In this approach, the inputs are the two images, I_1 and I_2, and both the recovered image as well as the deformation field are optimized, f and u. The label set becomes larger, for each possible recovered intensity, there is a possible translation of that pixel between both images, $(f_p; u_p) \in \mathcal{L}_f \cup \mathcal{L}_u$, e.g., $\mathcal{L}_f = \{(0; (-10; -10)), ..., (0; (+10; +10)), ..., (255; (-10; -10)), ..., (255; (+10; +10))\}$.

Energies for de-noising (Eq. 2) and for the recovery of the deformation field (Eq. 3) are combined in the same formulation and solved using the Graph Cuts optimization. The combined data term contains three terms. The

first, controlled by λ_{d_1}, measures how the recovered image, f, matches the image I_1. The second, controlled by λ_{d_2}, measures how the recovered image, f, matches the image I_2. The third, controlled by λ_{d_3}, measures how the data differs between the image I_1 and the image I_2 warped with the deformation field u:

$$\begin{aligned} D(f_p, u_p) &= \lambda_{d_1} D_{\text{de-noising}}(i_1(p), f(p)) \\ &+ \lambda_{d_2} D_{\text{de-noising}}(i_2(p+u_p), f(p)) \\ &+ \lambda_{d_3} D_{\text{registration}}(I_1(p), I_2(p+u_p)) \end{aligned} \quad (4)$$

The combined smoothness term contains two terms. The first, controlled by λ_{v_1}, measures how smooth the recovered image, f, is. The second, controlled by λ_{v_2}, measures how smooth the deformation field u is:

$$\begin{aligned} V(f_p, f_q, u_p, u_q) &= \lambda_{v_1} V_{\text{de-noising}}(f_p, f_q) \\ &+ \lambda_{v_2} V_{\text{registration}}(u_p, u_q). \end{aligned} \quad (5)$$

The data term (Eq. 4) and the smoothness term (Eq. 5) are used in the energy (Eq. 1). This way, both the recovered image f and the deformation field u is optimized simultaneously using the Graph Cuts framework. In the following results, the energy used is:

$$\begin{aligned} E(f,u) = & \\ & \sum_{p \in I_1, I_2} \left(\begin{array}{l} \lambda_{d_1}(i_1(p) - f_p)^2 + \\ \lambda_{d_2}(i_2(p+u_p) - f_p)^2 + \\ \lambda_{d_3}(i_1(p) - i_2(p+u_p))^2) \end{array} \right) \\ + & \sum_{p,q \in \mathcal{N}} \left(\begin{array}{l} \lambda_{v_1}|f_p - f_q| + \\ \lambda_{v_2}||u_p - u_q|| \end{array} \right). \end{aligned} \quad (6)$$

3. RESULTS

In the following experiments, a comparison is done between the de-noising of images, using the degraded image only, and using an additional image. The simultaneous approach is validated by trying to recover an image heavily corrupted by noise or missing data. Applications to brain MRI and cardiac MRI, CT and ultrasound images are presented to evaluate the improvement of using an additional image to remove the noise from a corrupted image.

3.1. Improving de-noising

The brain MRI shown in Fig. 1(b) is corrupted by a severe white noise, $N(\mu = 0, \sigma = 200)$. At full resolution (128×128), the head shape is barely recognized.

First, the noise removal using solely the image shown in Fig. 1(b) is done. The label set of possible recovered intensities is $\mathcal{L}_f = \{0, 1, ..., 255\}$. The minimization of the equation (Eq. 2), with parameters $\lambda = 0.5$, yields a poor result. The intensity difference between the original image (Fig. 1(a)) and the recovered image (Fig. 1(f)) is measured using the root mean square, which is $RMS = 63.10$. On the recovered image, the head silhouette can be discerned; however, details such as the ventricles or the skull are lost. Increasing the smoothness parameter λ will produce even coarser images, decreasing it will produce noisier images.

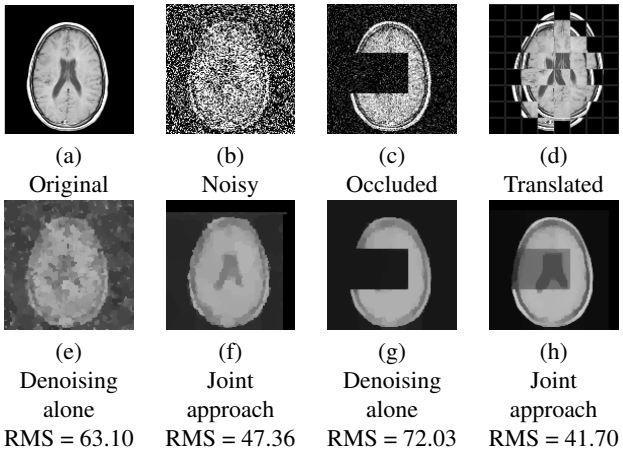

(a) Original (b) Noisy (c) Occluded (d) Translated

(e) Denoising alone RMS = 63.10 (f) Joint approach RMS = 47.36 (g) Denoising alone RMS = 72.03 (h) Joint approach RMS = 41.70

Fig. 1. (a) Original image, MRI brain scan, (b) degraded image, (c) with missing data, (d) checker board comparing the translated image witht he original image, (e) denoising alone of the degraded image, (f) joint approach enhancing the degraded image via registration of the translated image, (g) de-noising alone of the occluded image, (h) joint approach recovering the missing part in the occluded image via registration of the translated image.

Second, image de-noising is improved by registering an additional image (Fig. 1(d)). This new image is a translated version of the original image (comparison in Fig. 1(d)). The label set can contain a single deformation, that is the known translation $u_p \in \{(+10; +10)\}$, but to be closer to a real case scenario, all translations within a 3×3 window is also included. The label set used in this experiment is thus $\mathcal{L}_f \in \{f_p, u_p\}$, with $f_p \in \{0, 1, ..., 255\}$ and $u_p \in \{(+10; +10) + (+3; +3), ..., (-3; -3)\}$. In order to compare the joint de-noising and registration with the sole image de-noising, the same balance used in the previous experiment between data matching and smoothness is preserved, i.e., $\frac{1}{\lambda} = \frac{\lambda_{d_1}+\lambda_{d_2}+\lambda_{d_3}}{\lambda_{v_1}+\lambda_{v_2}}$. The parameters for equation (Eq. 6) are $\lambda_{d_1} = 0.33, \lambda_{d_2} = 0.33, \lambda_{d_3} = 0.36$ and $\lambda_{v_1} = 0.2, \lambda_{v_2} = 0.3$. The minimization removes the noise as shown in Fig. 1(e). The intensity difference between the original image and the image recovered with the joint approach (Fig. 1(f)) is decreased to $RMS = 47.39$. The head is clearly recognized, and details such as the ventricles are visible.

If the minimization favors the use of the second image with $\lambda_{d_2} \gg \lambda_{d_1}$, a similar effect to over fitting occurs. Fig. 1(g) shows image de-noising with $\lambda_{d_2} = 3.0$, and the minimization almost recreates the second image at the registered position.

3.2. Occlusions

In this second experiment, the degradation is pushed to an extreme; the method has to restore an image with missing data.

Fig. 1(c) shows the brain MRI with missing parts. A

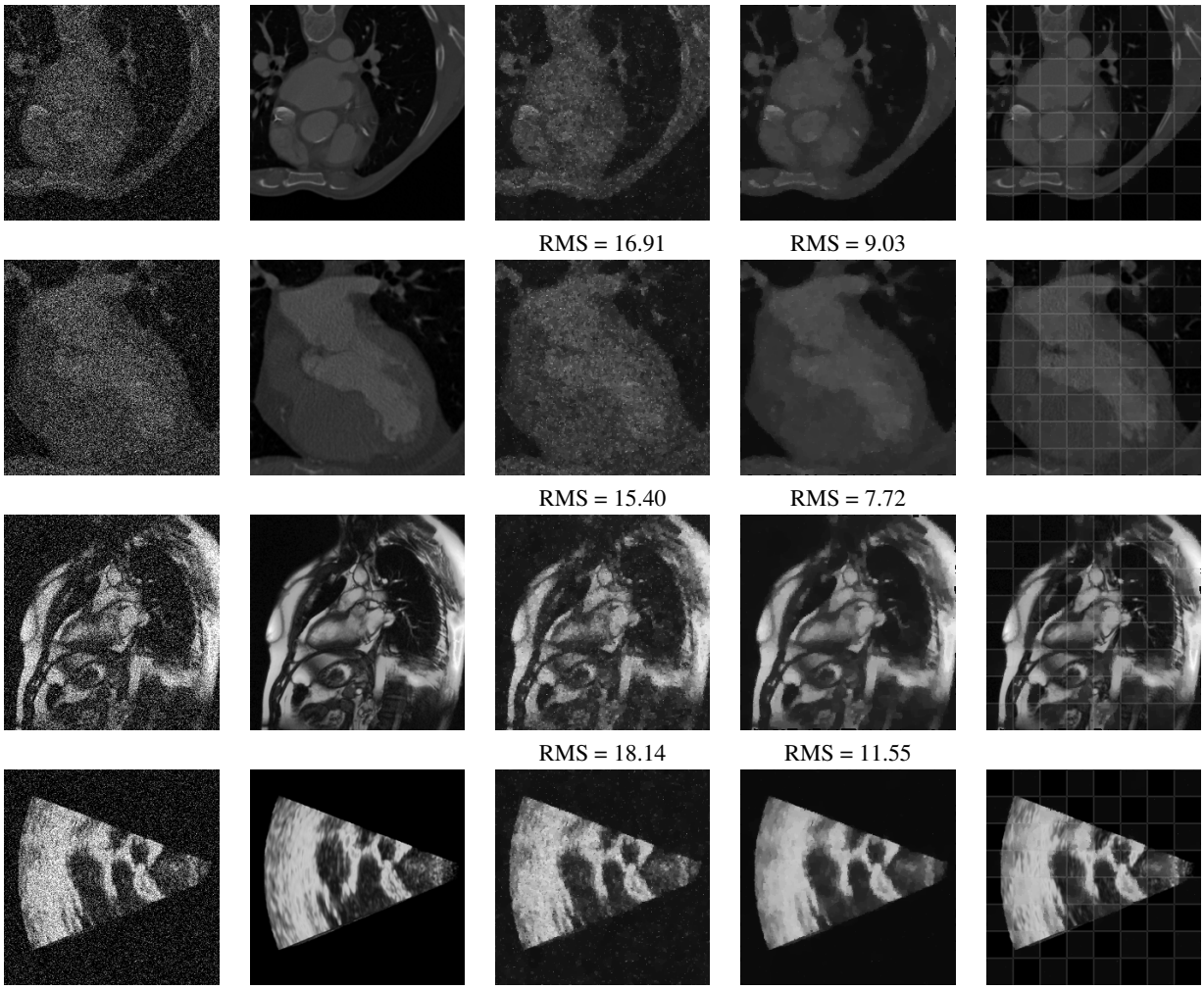

(a) Degraded image (b) Additional frame (c) De-noising alone (d) Joint approach (e) Ground truth vs. joint approach

Fig. 2. First and second row, image de-noising of a noisy cardiac CT frame; third row, image de-noising of a chest MRI; fourth row, image de-noising of a cardiac ultrasound frame: (a) Noisy frame, (b) additional frame, (c) image de-noising using only the noisy image, (d) image de-noising via registration of the second frame, and (e) its checkerboard comparison with the original frame.

white noise, $N(0, 50)$, is also added. As expected, removing noise using this image only cannot recover the missing data (Fig. 1(h)), the error is $RMS = 72.03$. However, when using an additional image, the missing information is restored by registering this second image, the error drops to $RMS = 41.70$. Fig. 1(f) shows the recovery of the missing part.

3.3. Recovery of Corrupted Frames

Medical image sequences are now becoming widely used in the cardiac field. This experiment evaluates the improvement in the quality of a corrupted frame by jointly registering an additional frame. Two images of the same slice, but taken at different time in the cardiac cycle, are shown on the first row of Fig. 2. One frame is purposely corrupted by a white noise, $N(0, 15)$. The label set contains all deformations within a 10×10 window, i.e., each pixel can move at most $(10; 10)$ pixels between the two frames.

The noise removal using only the first frame ($\lambda = 0.5$) yields the image (c) shown on the first row of Fig. 2. The mean square error with the original frame is $RMS = 16.91$. When using the registration of the second frame, the recovered image (Image (d) on the first row of Fig. 2) appears clearer, and the error drops to $RMS = 9.03$, this is a 46.6% improvement. In the joint approach, the ratio of the data over the smoothness energy is similar to the ratio used in the de-noising alone, that is, $\lambda_{d_1} = 0.33, \lambda_{d_2} = 0.33, \lambda_{d_3} = 0.36, \lambda_{v_1} = 0.8, \lambda_{v_2} = 0.7$.

The same experiment has been applied on a chest MRI (third row of Fig. 2). Image de-noising using only the degraded image shows an error of $RMS = 18.14$ with the original image. Noise removal is improved when using an additional image, the error drops to $RMS = 11.55$, this is a 36.3% improvement. Similarly, the same improve-

ment happens with a CT frame showing a cardiac ventricle (second row of Fig. 2). Image de-noising using only the degraded image yields an error of $RMS = 15.40$. The image quality is improved via the registration of a different frame, the error becomes $RMS = 7.72$, this is a 49.9% improvement. The last row of Fig. 2 shows the de-noising of a frame from a cardiac ultrasound sequence. When using only the degraded frame, the de-noising process yields an error of $RMS = 20.12$. Image de-noising via the registration of a different frame yields an error of $RMS = 14.05$ with the intensities of the original frame. This is a 30.17% improvement.

4. CONCLUSION

This paper shows that simultaneous image de-noising and image registration can be optimized via Graph Cut. The results show an improvement in the image enhancement when using a joint approach over the sole image de-noising, even in the presence of highly degraded images. The method has potential applications in the medical field where corrupted frames in a sequence can arise and would normally be discarded.

Other optimization methods exist, including variational approaches, however the Graph Cuts were chosen for its optimality. Our combined energy formulation is indeed solvable with the α-expansion algorithm. Future work will focus on a smoothness term preserving more efficiently discontinuities, thus handling the restoration in blurred images, and will use a more efficient deformation model for image registration. There is also an interest in using additional frames from different modalities. The work of Kim *et al.* [22], expressing Mutual Information in the Graph Cuts method, will be of great use.

Acknowledgments — We wish to thanks Siemens Corporate Research for help and support and the National Science and Engineering Research Council for funding.

5. REFERENCES

[1] B. J. Justusson, "Median filtering: Statistical properties," *Two Dimensional Digital Signal Processing*, vol. 2, pp. 161–196, 1981. 1

[2] S. Geman and D. Geman, "Stochastic relaxation, gibbs distributions, and the bayesian restoration of images," *IEEE Trans. on PAMI*, vol. 6, pp. 721–741, 1984. 1

[3] T. Chan and L. Vese, "An Active Contour Model without Edges," in *Int. Conf. on Scale-Space Theories in Computer Vision*, London, UK, 1999, pp. 141–151. 1

[4] S. Osher and L. I. Rudin, "Feature-oriented image enhancement using shock filters," *SIAM J. Numer. Anal.*, vol. 27, no. 4, pp. 919–940, August 1990. 1

[5] P. Perona and J. Malik, "Scale-space and edge detection using anisotropic diffusion," *IEEE Trans. on PAMI*, vol. 12, no. 7, pp. 629–639, July 1990. 1

[6] Y. Boykov, O. Veksler, and R. Zabih, "Fast approximate energy minimization via graph cuts," *IEEE Trans. on PAMI*, vol. 23, no. 11, pp. 1222–1239, 2001. 1, 2

[7] A. Raj and R. Zabih, "A graph cut algorithm for generalized image deconvolution," in *ICCV*, 2005, vol. 2, pp. 1048–1054. 1

[8] D. Cremers and L. Grady, "Statistical Priors for Efficient Combinatorial Optimization Via Graph Cuts," in *ECCV*, 2006, vol. 3953, pp. 263–274. 1

[9] J. C. Brailean and A. K. Katsaggelos, "Simultaneous recursive displacement estimation and restoration of image sequences," in *Int. Conf. on Systems, Man and Cybernetics*, 1992, pp. 1574–1579 vol.2. 1

[10] N. A. Woods, N. P. Galatsanos, and A. K. Katsaggelos, "Stochastic methods for joint registration, restoration, and interpolation of multiple undersampled images," *IEEE Transactions on Image Processing*, vol. 15, no. 1, pp. 201–213, Jan. 2006. 1

[11] P. Kornprobst, R. Deriche, and G. Aubert, "Image Sequence Restoration: A PDE Based Coupled Method for Image Restoration and Motion Segmentation," in *ECCV*, 1998, vol. 1407, pp. 548–562. 1

[12] J. Han, B. Berkels, M. Rumpf, J. Hornegger, M. Droske, M. Fried, J. Scorzin, and C. Shaller, "A variational framework for joint image registration, denoising and edge detection," in *Bildverarbeitung fur die Medizin*, 2006, pp. 246–250. 1

[13] A. Telea, T. Preußer, C. Garbe, M. Droske, and M. Rumpf, "A Variational Approach to Joint Denoising, Edge Detection and Motion Estimation," in *DAGM Symposium*, September 2006, vol. 4174, pp. 525–535. 1

[14] T. Preußer, M. Droske, C. Garbe, A. Telea, and M. Rumpf, "A phase field method for joint denoising, edge detection and motion estimation in image sequence processing," *SIAM Appl. Math.*, vol. 68, no. 3, pp. 599–618, 2007. 1

[15] T. Tang and A. Chung, "Non-rigid image registration using graph-cuts," in *MICCAI*, 2007, vol. 4791, pp. 916–924. 1

[16] R. So and A. Chung, "Multi-level non-rigid image registration using graph-cuts," in *Int. Conf. on Acoustics, Speech and Signal Proc.*, 2009, pp. 397–400. 1

[17] R. So and A. Chung, "Non-rigid image registration by using graph-cuts with mutual information," in *ICIP*. 2010, pp. 4429–4432, IEEE. 1

[18] R. So, T. Tang, and A. Chung, "Non-rigid image registration of brain magnetic resonance images using graph-cuts," *Pattern Recogn.*, vol. 44, pp. 2450–2467, Oct. 2011. 1

[19] P. Bhat, K. C. Zheng, N. Snavely, A. Agarwala, M. Agrawala, M. F. Cohen, and B. Curless, "Piecewise Image Registration in the Presence of Multiple Large Motions," in *CVPR*, June 2006, vol. 2, pp. 2491–2497. 1

[20] R. So and A. Chung, "Learning-based non-rigid image registration using prior joint intensity distributions with graph-cuts," in *ICIP*, 2011, pp. 709–712. 1

[21] H. Lombaert, Y. Sun, and F. Cheriet, "Landmark-based non-rigid registration via graph cuts," in *ICIAR*, Aug. 2007. 1

[22] J. Kim, V. Kolmogorov, and R. Zabih, "Visual correspondence using energy minimization and mutual information," in *ICCV*, October 2003, vol. 2, pp. 1033–1040. 2, 5